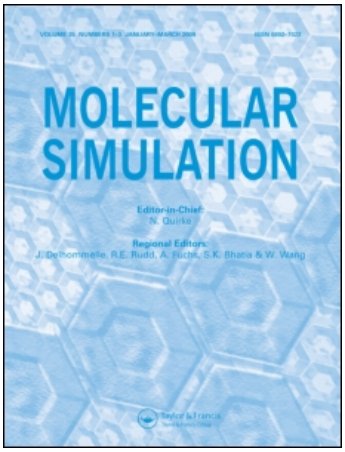

Molecular Simulation
Publication details, including instructions for authors and subscription information:
http://www.informaworld.com/smpp/title~content=t713644482

Density functional study of the electronic and optical properties of fluorene-thieno[3,2-*b*]thiophene-based conjugated copolymers

Zhijun Gong[ab]; Jolanta B. Lagowski[b]
[a] College of Chemistry and Environmental Engineering, Yangtze University, Jingzhou, Hubei, P.R. China [b] Department of Physics and Physical Oceanography, Memorial University of Newfoundland, St. John's, Newfoundland, Canada

To cite this Article Gong, Zhijun and Lagowski, Jolanta B.(2009) 'Density functional study of the electronic and optical properties of fluorene-thieno[3,2-*b*]thiophene-based conjugated copolymers', Molecular Simulation, 35: 9, 737 — 747
To link to this Article: DOI: 10.1080/08927020902833079
URL: http://dx.doi.org/10.1080/08927020902833079

Molecular Simulation
Vol. 35, No. 9, August 2009, 737–747

Taylor & Francis
Taylor & Francis Group

Density functional study of the electronic and optical properties of fluorene-thieno[3,2-*b*]thiophene-based conjugated copolymers

Zhijun Gong[ab] and Jolanta B. Lagowski[b]*

[a]*College of Chemistry and Environmental Engineering, Yangtze University, Jingzhou, Hubei 434023, P.R. China;* [b]*Department of Physics and Physical Oceanography, Memorial University of Newfoundland, St. John's, Newfoundland, Canada A1B 3X7*

(*Received 29 August 2008; final version received 16 February 2009*)

Quantum mechanical techniques are applied to investigate a family of π-conjugated copolymers: poly(9,9′-dimethylfluorene-*alt*-thiophene) (PFT), poly(9,9′-dimethylfluorene-*alt*-thieno[3,2-*b*]-thiophene) (PFTT), poly(9,9′-dimethylfluorene-*alt*-bithiophene) (PFT2), and poly(9,9′-dimethylfluorene-alt-α,α′-bisthieno[3,2-b]-thiophene) (PFTT2). Linear extrapolation is employed to obtain polymers' properties from oligomer calculations. That is, the HOMO–LUMO gaps (Δ_{H-L}s), band gaps (E_gs), ionisation potentials and electron affinities of the copolymers are obtained by plotting the corresponding quantities of the oligomers as a function of the inverse chain length ($1/n$) and extrapolating them to infinite chain length. The electronic properties of the neutral, positive and negative oligomers are determined using the density functional theory (DFT) at B3LYP/6-31G* approximation. The lowest singlet excitation energies of the oligomers of PFT, PFTT, PFT2, and PFTT2 are also determined with the use of the time-dependent DFT again at B3LYP/6-31G* approximation. Comparisons are made with experimental values when possible.

Keywords: fluorene; thiophene; DFT; band gaps; excitation energies

1. Introduction

Since the first demonstration of the electroluminescence (EL) from conjugated polymers such as poly(*p*-phenylene vinylene) [1], there has been great interest in developing full colour, flat panel displays using the (organic) polymer light emitting diodes (PLEDs) [2–4]. Many novel polymers have been synthesised to obtain materials with optimum photochemical characteristics. Among these materials, fluorene and thiophene based polymers have been shown to be promising candidates for the all-colour light-emitting materials. Their main advantage is that they show relatively high photoluminescence (PL) and EL quantum efficiencies, good solubility in organic solvents and thermal stability [5–7].

The electronic properties of a conjugated polymer are primarily governed by the chemical structure of its backbone. Quantum mechanical calculations can provide useful insight into the electronic and optical properties of known polymers and the prediction of properties of unknown polymers [8–13]. In the present work, we investigate four fluorene and thiophene based polymers: poly(9,9′-dimethylfluorene-*alt*-thiophene) (PFT) [5,14], poly(9,9′-dimethylfluorene-*alt*-thieno[3,2-*b*]-thiophene) (PFTT) [15–18], poly(9,9′-dimethylfluorene-*alt*-bithiophene (PFT2) [15–18], and poly(9,9′-dimethylfluorene-alt-α,α′-bisthieno[3,2-b]-thiophene) (PFTT2) [18] (see Figure 1). We estimate their energy band gaps with the oligomer extrapolation technique [9–11] using density functional theory (DFT).

In the extrapolation approach, the energy gaps are estimated in two ways: (1) from the difference between the highest occupied (HOMO) and lowest unoccupied (LUMO) molecular orbital eigen-energies (Δ_{H-L}); and (2) from the lowest singlet transition energies. In the first case, the HOMO–LUMO gaps can be compared to the electrochemical energy gaps as obtained with the use of cyclic voltammetry (CV) and, in the second case, the excitation energies can be compared to the optical gaps (E_gs) as obtained from PL experiments for example. The hole and electron extraction potentials (HEP and EEP) are also estimated [23,24]. In all cases, the energies of a sequence of increasingly longer oligomers are fitted to a line and then extrapolated to infinite chain length limit. This approach is an application of a well-known reciprocal rule for polymers which states that many properties of polymers tend to vary approximately linearly as functions of reciprocal chain lengths [19,20,22]. In summary, the main goal of this paper is to improve our understanding of how thiophene affects the optical and electronic properties of poly(fluorene) (PF), to illustrate how quantum mechanical modelling based on DFT can aid in the evaluation of ground- and excited-state properties of thiophene and fluorene based oligomers and

*Corresponding author. Email: jolantal@mun.ca

ISSN 0892-7022 print/ISSN 1029-0435 online

DOI: 10.1080/08927020902833079
http://www.informaworld.com

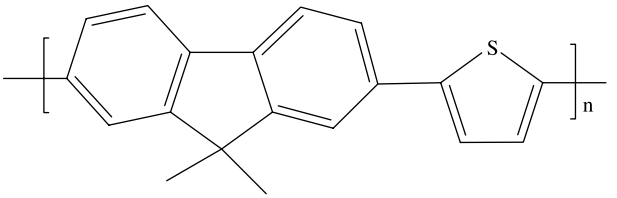

(FT)$_n$

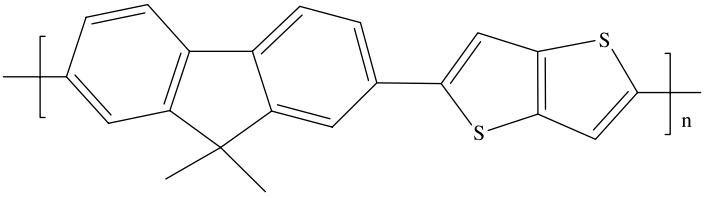

(FTT)$_n$

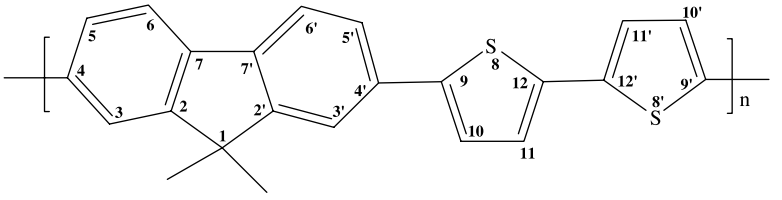

(FT2)$_n$

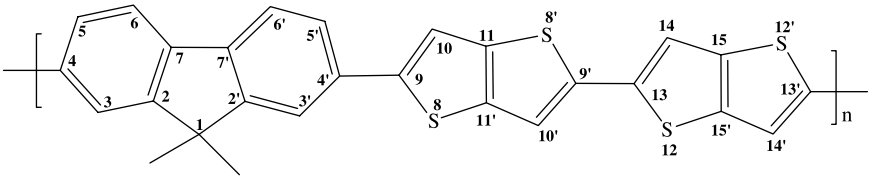

(FTT2)$_n$

Figure 1. Chemical structures of the systems studied.

polymers and to assess the accuracy of the two theoretical approaches to calculate band gaps by comparing them with the available experimental data.

2. Computational method

All calculations on oligomers ((FT)$_n$, (FTT)$_n$, (FT2)$_n$, and (FTT2)$_n$, $n = 1-4$) studied in this work have been performed using Gaussian 03 software package [21]. The electronic ground states of neutral, positive and negative oligomers were obtained by performing the DFT/B3LYP/6-31G* calculations. The transition energies were calculated at the ground-state geometries using TD-DFT/B3LYP/6-31G* approach. Ionisation potentials (IPs) and electron affinities (EAs) (both adiabatic and vertical) and EEPs and HEPs [23,24] of the oligomers were also obtained with DFT/B3LYP/6-31G* method as total energy differences. The corresponding copolymer (PFT, PFTT, PFT2, and PFTT2) energy band gaps were estimated from the HOMO–LUMO gaps and the lowest singlet excitation energies by applying the linear extrapolation technique to oligomer values. All linear extrapolations were performed using three values (corresponding to $n = 2-4$) of a given physical quantity. The correlation coefficient (often referred to as R^2) was determined to assess the accuracy of the linear fits. In all cases, the correlation coefficient was close to 1 (details are discussed below). Also the SE of estimate was either close to or less than 0.01 eV.

In all oligomer calculations, we substituted 9,9-dioctyl with 9,9-dimethyl in the fluorene rings to reduce the computation time. It has been shown that the length of the alkyl chains at the 9th position does not significantly affect the equilibrium geometries and hence does not effect the electronic and optical properties of the fluorene based

oligomers in vacuum [25]. The length of alkyl chains can affect the solubility and excimer formation in these systems [26,27].

3. Results and discussion

3.1. Ground-state structural properties

The chemical structures (and the labelling of atoms) of the systems studied are depicted in Figure 1. The B3LYP/6-31G* optimised structures of $(FT)_4$, $(FTT)_4$ and $(FT2)_4$ are shown in Figure 2. The selected optimised dihedral angles (such as $\Phi(5',4',9,8)$, $\Phi(11,12,12',8')$ and $\Phi(10',9',13,12)$) and bond lengths (such as $r(4',9)$, $r(12,12')$, $r(9',13)$) between the fluorene and thiophene based subunits of the oligomers are summarised in Table 1. As observed in other works [8] all systems are nonplanar. The dihedral angle between the two phenyl rings in the fluorene segment of all series of oligomers is fixed by

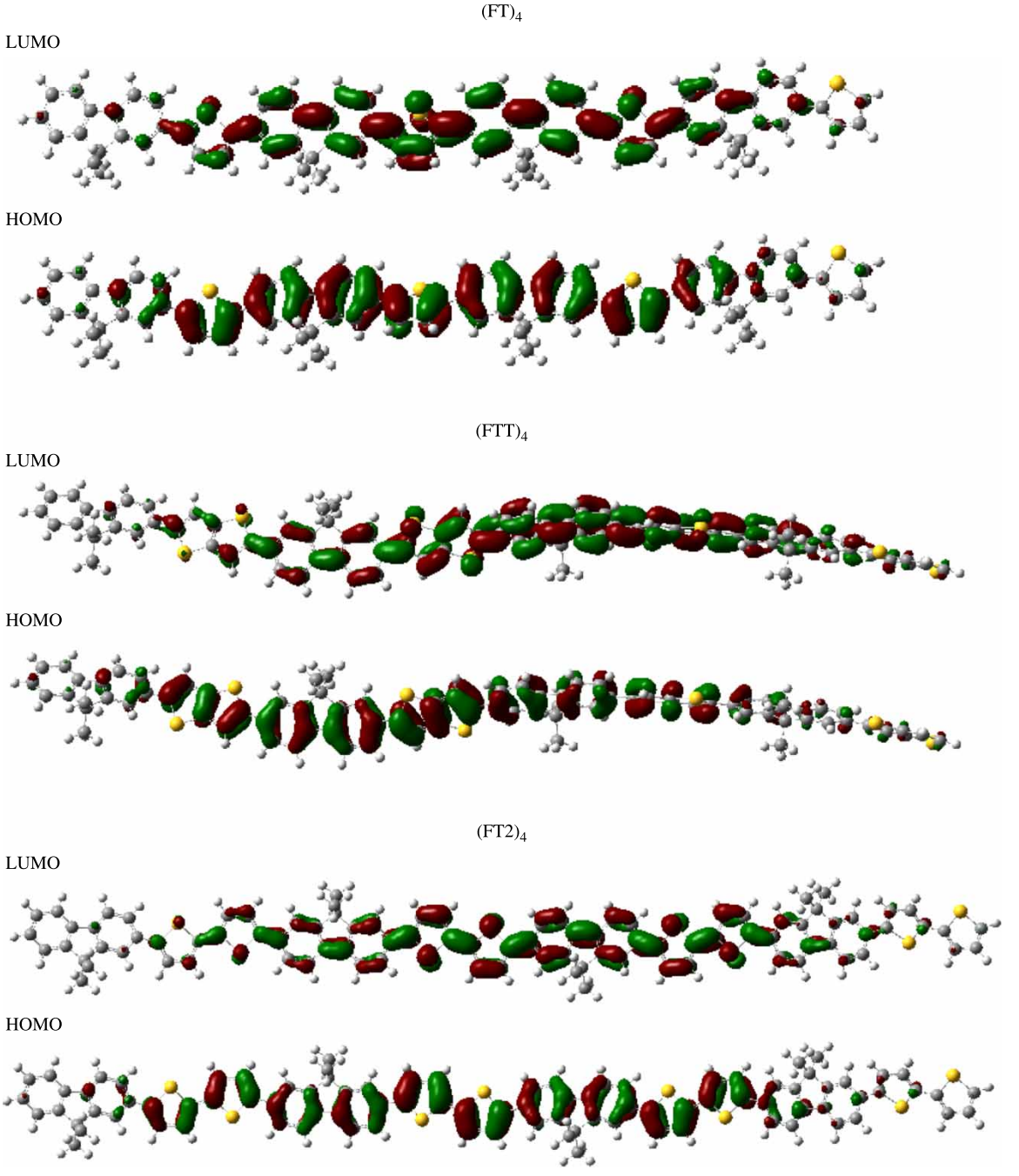

Figure 2. The contour plots of HOMOs and LUMOs of the $(FT)_4$, $(FTT)_4$ and $(FT2)_4$.

Table 1. Dihedral angles (between the planes containing the fluorene and thiophene moieties) and inter-ring distances of $(FT)_n$, $(FTT)_n$, $(FT2)_n$ and $(FTT2)_n$ ($n = 1–4$) obtained using B3LYP/6-31G* method.

Oligomer		F-T	T-F	F-T	T-F	F-T	T-F	F-T				
$(FT)_n$												
$n = 1$	Φ (deg)	27.9										
	r (Å)	1.468										
$n = 2$	Φ (deg)	26.6	26.0	27.5								
	r (Å)	1.465	1.465	1.467								
$n = 3$	Φ (deg)	27.5	24.7	25.0	27.0	27.5						
	r (Å)	1.465	1.465	1.465	1.465	1.467						
$n = 4$	Φ (deg)	27.2	24.8	26.3	25.7	24.9	26.9	27.7				
	r (Å)	1.465	1.465	1.465	1.465	1.465	1.465	1.467				
$(FTT)_n$												
$n = 1$	Φ (deg)	27.6										
	r (Å)	1.466										
$n = 2$	Φ (deg)	27.0	26.9	27.6								
	r (Å)	1.465	1.464	1.466								
$n = 3$	Φ (deg)	27.1	26.7	26.4	26.5	27.8						
	r (Å)	1.465	1.464	1.464	1.464	1.466						
$n = 4$	Φ (deg)	27.2	26.6	26.9	26.1	26.3	26.6	27.6				
	r (Å)	1.465	1.464	1.464	1.464	1.464	1.464	1.466				
Oligomer		F-T	T-T	T-F	F-T	T-T	T-F	F-T	T-T	T-F	F-T	T-T
$(FT2)_n$												
$n = 1$	Φ (deg)	26.6	19.2									
	r (Å)	1.465	1.448									
$n = 2$	Φ (deg)	25.3	17.7	24.5	25.8	18.9						
	r (Å)	1.464	1.445	1.464	1.464	1.448						
$n = 3$	Φ (deg)	25.8	16.4	24.9	25.2	15.8	26.1	25.2	19.3			
	r (Å)	1.464	1.445	1.464	1.464	1.445	1.464	1.464	1.448			
$n = 4$	Φ (deg)	26.1	15.0	25.1	26.0	13.4	26.4	25.3	17.7	25.3	25.6	18.9
	r (Å)	1.464	1.445	1.464	1.464	1.445	1.464	1.464	1.445	1.464	1.464	1.448
$(FTT2)_n$												
$n = 1$	Φ (deg)	27.0	18.4									
	r (Å)	1.465	1.445									
$n = 2$	Φ (deg)	26.7	16.2	25.3	26.4	18.6						
	r (Å)	1.464	1.444	1.464	1.464	1.445						
$n = 3$	Φ (deg)	27.1	17.2	25.7	26.4	17.5	26.8	26.0	19.8			
	r (Å)	1.464	1.444	1.464	1.464	1.444	1.464	1.464	1.445			
$n = 4$	Φ (deg)	27.8	18.2	27.2	26.0	16.5	25.3	25.7	17.3	26.4	26.6	19.1
	r (Å)	1.465	1.444	1.464	1.464	1.444	1.464	1.464	1.444	1.464	1.464	1.445

ring-bridged atoms and is no more than 1°. The largest dihedral angles in $(FT)_n$, $(FTT)_n$, $(FT2)_n$ and $(FTT2)_n$ are the inter-ring torsional angles between the fluorene and thiophene or the fluorene and thieno[3,2-*b*]-thiophene rings, which average round 26° in the middle of the oligomers. The torsional angles between the two adjacent thiophene or thieno[3,2-*b*]-thiophene rings in $(FT2)_n$ and $(FTT2)_n$ are smaller and their values range from 13° to 18°. The inter-ring distances are also remarkably consistent. The distance between fluorene and thiophene based ring is close to 1.464 Å (1.465 Å in $(FT)_n$) in nearly all systems in the middle part of the oligomer. The distance between two thiophene based rings is shorter and is 1.445 Å in $(FT2)_n$ and 1.444 Å in $(FTT2)_n$. In summary, the results of the optimised structures of the oligomers show that they have very similar ground state conformations. By ignoring the structural variations due to free ends, the structures of the corresponding polymers can be deduced which by extension must also be very similar in all four systems.

3.2. *Frontier molecular orbitals and energies*

In most conjugated organic materials, the lowest and the strongest electron dipole-allowed electron transitions with the largest oscillator strength (f) correspond almost exclusively to the promotion of an electron from the HOMO to the LUMO. In Figure 2, we have plotted

the contour plots of the B3LYP/6-31G* HOMOs and LUMOs of $(FT)_4$, $(FTT)_4$ and $(FT2)_4$. The electronic cloud distributions are similar in all four oligomers. The frontier orbitals spread over the π-conjugated backbones. As observed before, there is antibonding between the bridge atoms of the inter-ring, and bonding between the bridge carbon atom and its conjoint atoms of the intra-ring in the HOMO. By contrast, there is bonding in the bridge single bond of the inter-ring and antibonding between the bridge atom and its neighbour in the intra-ring in the LUMO. In general, the HOMOs possess antibonding character between the subunits. This explains the nonplanarity that is observed in the ground states of the oligomers. The bonding character between the two adjacent subunits in the LUMOs implies that the lowest singlet excited state structures should be more planar [8]. In addition, in the LUMOs the electronic clouds are extended to include the sulphur atoms as well as the carbon atoms along the backbone. For polymers, this implies that thiophene or thieno[3,2-*b*]-thiophene units serve as electron-accepting moieties that have high-electron affinity due to the presence of one or two electronegative heteroatoms in their respective co-monomers.

Efficient injection and transport of both holes and electrons are important parameters in the rational design of optimised devices such as light emitting diodes. These processes involve matching the frontier (HOMO and LUMO) energy levels of the organic material with the respective anode and cathode work functions. It is believed that electrochemical characterisation of polymers using CV gives the best experimental estimates of the HOMO and LUMO energies (the negative of which correspond to the IPs and EAs of the polymers) since it probes these states directly during the process of charge injection (holes into HOMO and electrons into LUMO) [15,17]. The experimental HOMO and LUMO energies (or equivalently IPs and EAs) are determined from an empirical formula that is based on the onset potentials of oxidation and reduction [15,17].

In Table 2, the polymer experimental values of IPs and EAs are compared with the B3LYP/6-31G* HOMO ($-\varepsilon_{\mathrm{HOMO}}$) and LUMO ($-\varepsilon_{\mathrm{LUMO}}$) extrapolated eigen-values (their correlation coefficients ranged from 0.9918 to 0.9998) for the respective polymers of $(FT)_n$, $(FTT)_n$, $(FT2)_n$ and $(FTT2)_n$. In this work, we consider the negative of the DFT HOMO and LUMO eigen values as approximate (theoretical) values for IPs and EAs. Strictly speaking, the Koopmans' theorem (that allows us to make this equivalence) does not hold for DFT orbital energies (except, $-\varepsilon_{\mathrm{HOMO}}$ is a good approximation to the corresponding IP). We justify the use of $-\varepsilon_{\mathrm{LUMO}}$ to approximate EA by pointing out that it has been used as in the past works (see also Ref. [10] for example). More importantly, we can see from Table 2 that the values of $-\varepsilon_{\mathrm{LUMO}}$ are in reasonable good agreement with the corresponding experimental EAs.

Table 2. Negative of the HOMO ($-\varepsilon_{\mathrm{HOMO}}$) and LUMO energies ($-\varepsilon_{\mathrm{LUMO}}$) (in eVs) of $(FT)_n$, $(FTT)_n$, $(FT2)_n$ and $(FTT2)_n$ obtained using B3LYP/6-31G* method.

Oligomer	$-\varepsilon_{\mathrm{HOMO}}$	$-\varepsilon_{\mathrm{LUMO}}$
$(FT)_n$		
$n = 1$	5.39	1.23
$n = 2$	5.04	1.65
$n = 3$	4.94	1.78
$n = 4$	4.90	1.83
$n = \infty$	4.76	2.02
Exp.	5.66[a]	2.00[a]
$(FTT)_n$		
$n = 1$	5.28	1.41
$n = 2$	5.00	1.78
$n = 3$	4.93	1.90
$n = 4$	4.90	1.95
$n = \infty$	4.80	2.12
Exp.	5.38[b], 5.27[c]	2.40[b], 2.58[c]
$(FT2)_n$		
$n = 1$	5.13	1.57
$n = 2$	4.90	1.88
$n = 3$	4.84	1.97
$n = 4$	4.82	2.01
$n = \infty$	4.74	2.14
Exp.	5.51[a], 5.41[b], 5.13[c]	2.06[a], 2.48[b], 2.54[c]
$(FTT2)_n$		
$n = 1$	5.03	1.81
$n = 2$	4.87	2.05
$n = 3$	4.84	2.12
$n = 4$	4.82	2.15
$n = \infty$	4.77	2.25
$(Fluorene)_n$		
$n = 1$	5.73	0.74
$n = 2$	5.33	1.21
$n = 3$	5.19	1.38
$n = 4$	5.13	1.46
$n = \infty$	4.93	1.71
Exp.	5.7[d] (CV), 5.75[d] (UPS/IPES)	2.1[d] (CV), 2.50[d] (UPS/IPES)

[a] [14] (film). [b] [15] (film). [c] [17] (chloroform solution). [d] [28] (film).

Also, it should be noted that experimental EAs are often calculated by subtracting IPs from band gaps (i.e. EA = E_g − IP or E_g = IP − EA) and since E_gs, in our case, are estimated by HOMO–LUMO gaps ($\Delta_{\mathrm{H-L}}$s) then it is not unreasonable to approximate EA by $-\varepsilon_{\mathrm{LUMO}}$ and IP by $-\varepsilon_{\mathrm{HOMO}}$.

As can be seen from Table 2, experimental IPs and EAs vary depending on the sample preparation. Typically, the IPs obtained from films (solid state) of polymers are larger than those obtained in (chloroform) solution. Solid state IPs also depend on the film preparation, for example for FTT2 polymer there are two possible values for its IP: 5.41 eV [15] and 5.51 eV [14]. In contrast, the EAs of the film samples are smaller than those obtained in solution (the solution stabilises the negative ion). For comparison

purposes we also include the DFT and experimental [28] energies for PF. While the experimental methods may give slightly different values for IPs and EAs, the computational trends are quite clear. PFT, PFTT, PFT2 and PFTT2 all give smaller IPs and larger EAs than those computed for PF, indicating that both the hole and electron injections would be improved in these materials relative to PF. The lowest IP has been calculated in PFT2 (4.74 eV) followed by PFT (4.76 eV), PFTT2 (4.77 eV) and PFTT (4.80 eV). This suggests that the introduction of thiophene rings will contribute more to the hole-injection performance than that of the thieno[3,2-*b*]-thiophene groups. The highest EA has been calculated in PFTT2 (2.25 eV) followed by PFT2 (2.14 eV), PFTT (2.12 eV) and PFT (2.02 eV). These trends indicate that it would be difficult to make a single material that is equally good for both hole and electron injection/transport. PFTT2 seems to be the best material with good balance for both hole and electron transport. In general, the DFT eigen-value trends agree well with the experimental trends for EAs but not for IPs and the values of the $-\varepsilon_{HOMO}$s are poorer estimates of IPs than $-\varepsilon_{LUMO}$s of EAs at the B3LYP/6-31G* approximation.

Table 3. Ionisation potentials, electron affinities, and HEP and EEP for each oligomer ($n = 1$–4) as indicated and their respective polymers ($n = \infty$) (in eV).

Oligomer	IP (*v*)	IP (*a*)	HEP	EA (*v*)	EA (*a*)	EEP
(FT)*n*						
$n = 1$	6.83	6.64	6.49	-0.18	0.018	0.17
$n = 2$	6.07	5.93	5.79	0.63	0.80	0.95
$n = 3$	5.78	5.66	5.55	0.95	1.09	1.22
$n = 4$	5.60	5.52	5.44	1.14	1.24	1.34
$n = \infty$	5.15	5.11	5.09	1.64	1.68	1.74
$(FTT)_n$						
$n = 1$	6.62	6.44	6.30	0.096	0.29	0.44
$n = 2$	5.95	5.81	5.67	0.85	1.01	1.15
$n = 3$	5.68	5.58	5.48	1.14	1.27	1.38
$n = 4$	5.53	5.45	5.38	1.31	1.41	1.50
$n = \infty$	5.12	5.10	5.09	1.76	1.81	1.85
$(FT2)_n$						
$n = 1$	6.42	6.23	6.08	0.31	0.51	0.66
$n = 2$	5.79	5.67	5.55	0.99	1.14	1.27
$n = 3$	5.54	5.46	5.37	1.26	1.37	1.47
$n = 4$	5.40	5.34	5.28	1.42	1.50	1.58
$n = \infty$	5.02	5.02	5.01	1.84	1.85	1.89
$(FTT2)_n$						
$n = 1$	6.18	6.01	5.87	0.68	0.87	1.01
$n = 2$	5.65	5.54	5.44	1.28	1.40	1.52
$n = 3$	5.44	5.36	5.29	1.51	1.60	1.68
$n = 4$	5.32	5.26	5.20	1.64	1.71	1.78
$n = \infty$	5.00	4.98	4.97	1.99	2.02	2.03
$(Fluorene)_n$						
$n = 1$	7.41	7.28	7.14	-0.89	-0.73	-0.57
$n = 2$	6.55	6.42	6.29	0.01	0.19	0.36
$n = 3$	6.19	6.08	5.98	0.39	0.54	0.68
$n = 4$	5.99	5.90	5.82	0.60	0.72	0.84
$n = \infty$	5.44	5.38	5.35	1.18	1.25	1.32

The suffixes (*v*) and (*a*), respectively, indicate vertical and adiabatic values obtained using B3LYP/6-31G* method.

3.3. *Ionisation potentials and electron affinities – Total energy differences approach*

Another way of computing IPs and EAs is to use the total energy difference approach which involves the computation of the total energies for the neutral and positive and negative ions and subsequently their respective differences. Both vertical (*v*, at the geometry of the neutral molecule) and adiabatic (*a*, optimised geometries for both the neutral and charged molecule) values of IPs and EAs were obtained and are listed in Table 3 (the correlation coefficients for the extrapolated values ranged from 0.9967 to 1.0000). As can be clearly seen from the table (B3LYP/6-31G*) energy difference approach gives better agreement with experimental values for IPs but not for EAs. All values of IPs are larger than (or are very close to) 5 eV and are on the average 0.3 eV higher than $-\varepsilon_{HOMO}$s. However, all values of EAs as obtained from energy differences decrease by 0.25 eV and hence increase their discrepancy with the respective experimental values. If, as discussed above, IPs and EAs are used to estimate the energy barriers for the injection of both holes and electrons into the polymer, then the trends predicted by Table 3 are different (and somewhat simpler) than those obtained from Table 2 data. In particular, PFTT2 has the lowest IP (4.98 eV) and highest EA (2.02 eV) of all compounds studied followed by PFT2, PFTT and PFT. Since the total energy difference method is typically considered a more accurate estimate of the respective IPs and EAs, it is expected that these values and their trends would be more reflective of the physical systems. This approach clearly predicts that PFTT2 would be the best material for both hole and electron injections from the typical anode (ITO) and cathode (Ca or Al), respectively. PFT2 should also be a good candidate.

A more direct way of estimating the hole and electron injection capability of a given material is to determine HEPs and EEPs. Their values are included in Table 3. HEPs and EEPs are determined from the total energy differences between positive or negative ions and neural oligomers computed using their respective ion geometries. Once again PFTT2 shows the lowest HEP (4.97 eV which is lower by 0.5 eV in comparison to PF [24])) and highest EEP (2.03 eV which is higher by 0.8 eV in comparison to PF [24]) relative to other systems (PFT2 has similar values (5.02 and 1.89 eV, respectively)). These results confirm again that both PFTT2 and PFT2 would be good candidates for materials that should have both good hole and electron injection and transport capabilities. It appears that the presence of the additional heteroatoms (S) in bithiophene and bisthieno[3,2-*b*]-thiophene and longer effective conjugation lengths plays a role in obtaining

these capabilities. In practice there are other obstacles that must be overcome before these materials could be used optimally [16,18].

3.4. Polymer band gap estimates

Two theoretical approaches are used in this paper for estimating energy gaps of the polymers. One way is based on the ground state properties of oligomers, from which the energy gap is estimated from the energy difference between the HOMO and LUMO eigen-energies plotted as function of $1/n$ and extrapolated to $n = \infty$ (termed the HOMO–LUMO gaps (Δ_{H-L}s)). The implicit assumption underlying this approximation is that the lowest singlet excited state can be described by only one singly excited configuration in which an electron is promoted from HOMO to LUMO. Experimentally, it is known that an accurate description of the lowest singlet excited state requires a linear combination of a number of excited configurations, although the one mentioned above often plays a dominant role. The TD-DFT methodology which has this functionality (it also includes in its formalism the electron correlation effects) is employed to extrapolate energy gap of polymers from the calculated first dipole-allowed excitation energy (E_g) of their oligomers. The energy gap results are presented in Table 4, where Δ_{H-L}s and lowest singlet excited energies (E_gs) obtained by TD-DFT are listed. The calculated Δ_{H-L} and E_g values are also plotted in Figure 3 as function of inverse chain length. All curves extrapolate linearly to the $n = \infty$ limit. The extrapolated ($n = \infty$) values are also given in Table 4. The correlation coefficients of these extrapolated values range from 0.9967 to 1.0000, again indicating very good linear fits.

In most cases, for a given polymer one can obtain (similar to IPs and EAs) number of experimental values for a band gap. There are obvious differences between the band gaps determined from electrochemical and spectroscopic and/or optical means. Electrochemically determined band gaps appear to give larger values than those obtained through optical (UV–vis spectrum) means. The morphology (film or solution) of the material also plays a role. Band gaps obtained in the film are higher than those obtained in the (chloroform) solution. The values for optical bands also depend on whether the absorption onset or the maximum wavelength (λ_{max}) is used. E_g obtained from λ_{max} gives values that are larger by approximately 0.3 eV in comparison to those determined from the

Table 4. The HOMO–LUMO gaps (Δ_{H-L}) and the lowest excitation energies (E_g) of $(FT)_n$, $(FTT)_n$, $(FT2)_n$, $(FTT2)_n$ and their respective polymers ($n = \infty$) (all energies in eVs).

Oligomer	Δ_{H-L}	E_g (TD-B3LYP/6-31G*)
$(FT)_n$		
$n = 1$	4.16	3.87
$n = 2$	3.39	3.04
$n = 3$	3.16	2.79
$n = 4$	3.07	2.68
$n = \infty$	2.74	2.31
Exp.	3.66[a]	2.83[a]
$(FTT)_n$		
$n = 1$	3.88	3.59
$n = 2$	3.22	2.88
$n = 3$	3.03	2.66
$n = 4$	2.95	2.57
$n = \infty$	2.67	2.25
Exp.	2.98[b], 2.69[c]	2.63[b], 2.88[c]
$(FT2)_n$		
$n = 1$	3.56	3.28
$n = 2$	3.02	2.67
$n = 3$	2.87	2.50
$n = 4$	2.81	2.43
$n = \infty$	2.59	2.18
Exp.	3.45[a], 2.93[b], 2.49[c]	2.90[a], 2.59[b], 2.73[c]
$(FTT2)_n$		
$n = 1$	3.23	2.97
$n = 2$	2.82	2.49
$n = 3$	2.72	2.37
$n = 4$	2.67	2.32
$n = \infty$	2.52	2.15
$(Fluorene)_n$		
$n = 1$	4.99	4.62
$n = 2$	4.11	3.75
$n = 3$	3.81	3.41
$n = 4$	3.67	3.26
$n = \infty$	3.23	2.76
Exp.	3.6[d] (CV), 3.2–3.48[e]	3.15[b], 3.3[d] (UPS/IPES), 3.25[e], 3.27[f]

[a] [14] (film). [b] [15] (film). [c] [17] (chloroform solution). [d] [28] (film). [e] [29] (film). [f] [27]. (E_g(exp) are obtained at the λ_{max} from the UV–vis absorption spectral data).

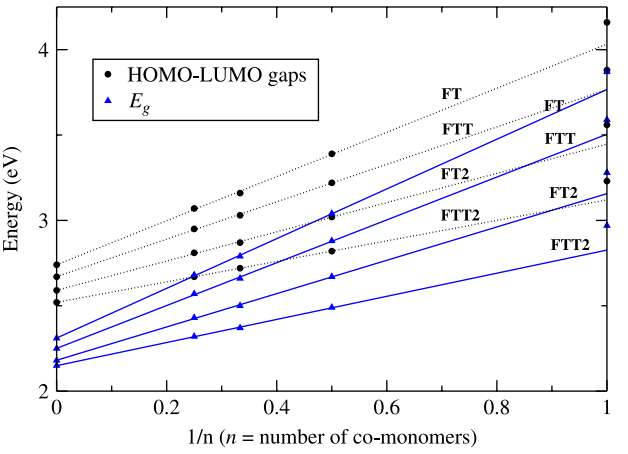

Figure 3. The HOMO–LUMO gaps (B3LYP/6-31G*) and the lowest excitation energies E_gs (TD-DFT/B3LYP/6-31G*) plotted as a function of reciprocal chain length n for $(FT)_n$, $(FTT)_n$, $(FT2)_n$ and $(FTT2)_n$ ($n = 1$–4) (in each case solid and dotted lines are linear fits to $n = 2$–4 points).

Table 5. Electronic transition data obtained using TD-DFT/B3LYP/6-31G* for $(FT)_n$.

Electronic transition	Wavelengths (nm)	f	MO/character
$(FT)_1$			
$S_1 \rightarrow S_0$	320.71	0.8451	HOMO → LUMO(+84%)
$S_2 \rightarrow S_0$	283.88	0.0001	HOMO → LUMO + 1(+70%)
			HOMO − 4 → LUMO(+11%)
			HOMO − 3 → LUMO(+11%)
$(FT)_2$			
$S_1 \leftarrow S_0$	407.45	2.0584	HOMO → LUMO(+88%)
$S_2 \leftarrow S_0$	344.63	0.0053	HOMO − 1 → LUMO(+48%)
			HOMO → LUMO + 1(50%)
$(FT)_3$			
$S_1 \leftarrow S_0$	444.72	3.1671	HOMO → LUMO(+88%)
$S_2 \leftarrow S_0$	384.65	0.0068	HOMO − 1 → LUMO (+66%)
			HOMO → LUMO + 1(+31%)
$(FT)_4$			
$S_1 \leftarrow S_0$	462.21	4.2762	HOMO → LUMO(+86%)
$S_2 \leftarrow S_0$	412.43	0.0081	HOMO − 1 → LUMO(+53%)
			HOMO → LUMO + 1(+34%)

onset wavelength. It is usually believed that experimental λ_{max} values give the appropriate comparison with the computational discrete E_gs since they are computed for isolated gas-phase single chains. These discrete values would typically be broadened in either film or solution environment with the peak of the broadened absorption spectrum corresponding to the discrete gas-phase value.

The computational results given in Table 4, all show the same trend, namely all estimates of band gaps for polymers containing thiophene moieties are smaller than the one obtained for PF. The narrower band gaps of PFT, PFTT, PFT2 and PFTT2 would lead to the longer absorption and emission wavelengths relative to PF. PFFT2 gives the smallest band gap (the two estimates are 2.52 and 2.15 eV) followed by PFT2, PFTT and PFT. This trend clearly correlates with the decreasing effective conjugation length as one goes from PFTT2 to PFT (see Figure 2). Comparison between computational estimates of band gaps and the experimental values indicate that the best estimates are obtained with Δ_{H-L}s. This is a fortuitous result due to error cancellation that does not occur to the same extent for the excitation energy method. Another factor to consider while making these comparisons, is that solid-state effects (like polarisation effects and intermolecular packing forces) are neglected in the gas-phase calculations. These interactions result in a decreased interring twist and consequently a reduced gap (by 0.2–0.3 eV) in a thin film or solution compared to an isolated molecule. If this effect was to be taken into account, then the

Table 6. Electronic transition data obtained using TD-DFT/B3LYP/6-31G* for $(FTT)_n$.

Electronic transition	Wavelengths (nm)	f	MO/character
$(FTT)_1$			
$S_0 \rightarrow S_1$	345.25	1.0784	HOMO → LUMO(+84%)
$S_0 \rightarrow S_2$	290.70	0.0056	HOMO → LUMO + 1(+41%)
			HOMO → LUMO + 2(20%)
			HOMO − 1 → LUMO(+17%)
$(FTT)_2$			
$S_1 \leftarrow S_0$	431.21	2.5120	HOMO → LUMO(+88%)
$S_2 \leftarrow S_0$	367.42	0.0196	HOMO − 1 → LUMO(+56%)
			HOMO → LUMO + 1(42%)
$(FTT)_3$			
$S_1 \leftarrow S_0$	465.95	3.8191	HOMO → LUMO(+88%)
$S_2 \leftarrow S_0$	406.42	0.0280	HOMO − 1 → LUMO(+91%)
$(FTT)_4$			
$S_1 \leftarrow S_0$	481.64	5.1650	HOMO → LUMO(+83%)
$S_2 \leftarrow S_0$	435.60	0.0152	HOMO − 1 → LUMO(+52%)
			HOMO → LUMO + 1(+34%)

Table 7. Electronic transition data obtained using TD-DFT/B3LYP/6-31G* for $(FT2)_n$.

Electronic transition	Wavelengths (nm)	f	MO/character
$(FT2)_1$			
$S_1 \leftarrow S_0$	378.07	1.2223	HOMO → LUMO(+84%)
$S_2 \leftarrow S_0$	311.77	0.0007	HOMO → LUMO + 1(+59%)
			HOMO − 1 → LUMO(+39%)
$(FT2)_2$			
$S_1 \leftarrow S_0$	464.13	2.7122	HOMO → LUMO(+88%)
$S_2 \leftarrow S_0$	398.95	0.0108	HOMO − 1 → LUMO(+54%)
			HOMO → LUMO + 1(44%)
$(FT2)_3$			
$S_1 \leftarrow S_0$	495.47	4.0838	HOMO → LUMO(+85%)
$S_2 \leftarrow S_0$	437.65	0.0847	HOMO − 1 → LUMO(+62%)
			HOMO → LUMO + 1(24%)
$(FT2)_4$			
$S_1 \leftarrow S_0$	509.68	5.4738	HOMO → LUMO(+79%)
$S_2 \leftarrow S_0$	466.92	0.1897	HOMO − 1 → LUMO(+46%)
			HOMO → LUMO + 1(38%)

discrepancy between the theory and experiment could even be larger.

3.5. *Absorption spectra of oligomers*

The TD-DFT//B3LYP/6-31G* has been used to obtain the energies of the first five singlet excited states of the four series of oligomers performed on their ground-state equilibrium geometries. Their absorption wavelengths, oscillator strengths and excitation character are listed in Tables 5–8 (for sake of brevity, only the data for the lowest two singlet excited states are given in Tables 5–8). All electronic transitions are of the $\pi-\pi^*$ type and involve both subunits of the co-monomers. That is, no localised electronic transitions are obtained among the first five singlet–singlet transitions. In each oligomer of the four series, excitation to the S_1 state corresponds almost exclusively to the promotion of an electron from the HOMO to the LUMO. The excitation energies of the next four states have relatively small *f*s, the *f*s of $S_0 \rightarrow S_1$ electronic transition are the largest. Furthermore, the oscillator strength coupling the lowest charge-transferred $\pi-\pi^*$ singlet excited state to the ground state increases by about one order of magnitude upon adding one repeat unit to the co-monomers of PFT, PFTT, PFT2 and PFTT2. Another trend is related to the effective conjugation lengths, the absorption wavelengths and the *f*s of $S_0 \rightarrow S_1$ electronic transition progressively increase as the effective conjugation increases from FT, FTT, FT2 to FTT2 oligomers (the corresponding band gaps decrease).

From Tables 5–8 we find that our calculated TD-DFT values of the absorption λ_{max} overestimate the experimental λ_{max} values. For the short oligomers such as $(FT)_1$ there are indications [8] that discrepancy between the

Table 8. Electronic transition data obtained using TD-DFT/B3LYP/6-31G* for $(FTT2)_n$.

Electronic transition	Wavelengths (nm)	f	MO/character
$(FTT2)_1$			
$S_1 \leftarrow S_0$	417.97	1.7463	HOMO → LUMO(+83%)
$S_2 \leftarrow S_0$	343.44	0.0005	HOMO → LUMO + 1(+57%)
			HOMO − 1 → LUMO(+42%)
$(FTT2)_2$			
$S_1 \leftarrow S_0$	497.05	3.6474	HOMO → LUMO(+87%)
$S_2 \leftarrow S_0$	432.57	0.0354	HOMO − 1 → LUMO(+63%)
			HOMO → LUMO + 1(+34%)
$(FTT2)_3$			
$S_1 \leftarrow S_0$	522.38	5.5039	HOMO → LUMO(+81%)
$S_2 \leftarrow S_0$	471.06	0.0930	HOMO − 1 → LUMO(+55%)
			HOMO → LUMO + 1(31%)
$(FTT2)_4$			
$S_1 \leftarrow S_0$	534.65	7.3945	HOMO → LUMO(+74%)
$S_2 \leftarrow S_0$	496.69	0.0500	HOMO − 1 → LUMO(+44%)
			HOMO → LUMO + 1(+38%)

theory and experiment is less than 20 nm. For the longer oligomers and polymers, this discrepancy grows to closer to 100 nm. For example, (using data from Table 4), for PFT, PFTT and PFT2, the theoretical λ_{max}s are predicted to be 537, 551, 569, respectively. This should be compared with respective experimental values: 438 nm (film), [14] 448 nm (film) and 458 nm (film) [16]. Many investigations show that TD-DFT is a good predictive tool for absorption spectra of molecules. However, this method does not work as well for the extended systems [30].

3.6. The properties of excited structures and the emission spectra

The relaxed excited state structures are typically obtained using the configuration interaction singles (CIS) method. The CIS method is computationally very intensive for large molecular systems such the ones studied in the paper. In our previous work [8], we obtained fully optimised CIS/6-31G* structures of monomers of PFT, PFTT, PFT2 and PFTT2. The main conclusions of that work was that in their (relaxed) lowest singlet excited states all monomers become nearly planar and more rigid as the inter-ring bonds are shortened and compounds become more quinoidal or benzoic-like. When TD-DFT/B3LYP/6-31G* calculations were performed [8] on the monomers' optimised CIS geometries, their emission wavelengths could be estimated for the lowest singlet excited states. They were calculated to be 369 nm (FT), 396 nm (FTT), 439 nm (FT2) and 474 nm (FTT2). When these values are compared with the corresponding data in Tables 5–8, one notes that the emission wavelengths are red-shifted between 50 and 60 nm relative to the absorption λ_{max}s (49, 51, 61 and 56 nm for FT, FTT, FT2 and FTT2, respectively). These theoretical/computational predictions agree well with experimental data which give differences of the order of 40–60 nm between the maximum of the absorption peak and the maximum of the first vibronic fluorescence (emission) peak. These values are similar for both the monomers and polymers in both the thin film and solution environment [14,16,25]. For example, for PFTT, the differences are 39 nm (solution) and 47 nm (film) and for PFT2, they are 42 nm (solution) and 53 nm (film) [16]. This good agreement suggests that the excited structures of PFT, PFTT, PFT2 and PFTT2 and their oligomers have a strong coplanar tendency which, in turn, lengthens the effective conjugation along the backbone and decreases the band gaps. In addition, based on the above results, we conclude that both absorption and emission wavelengths must be overestimated by the same amount (approximately 100 nm for polymers, less for shorter oligomers) when using the TD-DFT/B3LYP/6-31G* method since the difference between them remains constant (average 50 nm) when going from monomers to polymers. This means that the emission wavelength for PFTT2 is of the order of 527 nm ($= 577 - 100 + 50$ nm) which is indicative of greenish yellow light emission in PL experiments (similar to PFTT and PFT2) [16].

4. Conclusions

All the oligomers investigated show non-planar structures in their ground states. All top molecular orbitals are delocalised on both subunits of the oligomers. The HOMOs possess an antibonding character between subunits, which may explain the non-planarity in their ground states. On the other hand, the LUMOs show bonding character between the two adjacent rings, in agreement with the more planar S_1 excited state. The combination of thiophene or thieno[3,2-*b*]-thiophene with the fluorine moieties resulted in the reduced LUMO energies and consequently the electron injection was greatly improved. Excitation to the S_1 state corresponds almost exclusively to the promotion of an electron from the HOMO to the LUMO. Accordingly, the energy of the $S_0 \rightarrow S_1$ electronic transition follows the HOMO–LUMO energy gap of each oligomer. The first electronic transition gives rise to largest values of the oscillator strength in each oligomer. The red-shift in absorption and emission spectra of PFTT2 compared with PFT2 is attributed to an increase of polymer chain planarity and effective conjugation length. We predict an absorption and emission wavelengths of the order of 480 and 530 nm, respectively, for PFTT2. This study indicates that a rational design of the tunable light-emitting fluorine derivatives and related polymers is possible and should contribute to the development of organic light-emitting diodes.

Acknowledgements

This work was supported in part by the Natural Science and Engineering Research Council of Canada (NSERC) and the Visiting Scholarship Research Foundation of Yangtze University. Calculations were performed on computers at the Atlantic Computational Excellence Network (ACEnet) computational resources.

References

[1] J.H. Burroughes, D.D.C. Bradley, A.R. Brown, R.N. Marks, K. Mackay, R.H. Friend, P.L. Burns, and A.B. Holmes, *Light-emitting diodes based on conjugated polymers*, Nature 347 (1990), pp. 539–541.

[2] D. Braun and A. Heeger, *Visible light emission from semiconducting polymer diodes*, J. Appl. Phys. Lett. 58 (1991), pp. 1982–1984.

[3] J.R. Sheats, H. Antoniadis, M. Hueschen, W. Leonard, J. Miller, R. Moon, D. Roitman, and A. Stocking, *Organic electroluminescent devices*, Science 273 (1996), p. 884.

[4] V. Savvateev, A. Yakimov, and D. Davidov, *Transient electroluminescence from poly(phenylenevinylene)-based devices*, Adv. Mater. 11 (1997), pp. 519–531.

[5] B. Tsuie, J.L. Reddinger, G.A. Sotzing, J. Soloducho, A.R. Katritzky, and J.R. Reynolds, *Electroactive and luminescent polymers: new fluorene-heterocycle-based hybrids*, J. Mater. Chem. 26 (1999), p. 2501.

[6] J. Pei, W.-L. Yu, W. Huang, and A.J. Heeger, *The synthesis and characterization of an efficient green electroluminescent conjugated polymer: poly[2,7-bis(4-hexylthienyl)-9,9-dihexylfluorene]*, Chem. Commun. 17 (2000), pp. 1631–1632.

[7] B. Liu, W.-L. Yu, Y.-H. Lai, and W. Huang, *Synthesis, characterization, and structure-property relationship of novel fluorene-thiophene-based conjugated copolymers*, Macromolecules 33 (2000), pp. 8945–8952.

[8] Z. Gong and J.B. Lagowski, *Singlet cxcitation energies of thiophene derivatives of fluorene: TD-DFT study*, Int. J. Quan. Chem. 107 (2007), pp. 159–171.

[9] O. Kwon and M.L. McKee, *Theoretical calculations of band gaps in the aromatic structures of polythieno[3,4-b]benzene and polythieno[3,4-b]pyrazine*, J. Phys. Chem. A 104 (2000), pp. 7106–7112.

[10] U. Salzner, J.B. Lagowski, P.G. Pickup, and R.A. Poirier, *Comparison of geometries and electronic structures of polyacetylene, polyborole, polycyclopentadiene, polypyrrole, polyfuran, polysilole, polyphosphole, polythiophene, polyselenophene and polytellurophene*, Synth. Metals 96 (1998), pp. 177–189.

[11] J. Ma, S. Li, and Y. Jiang, *A time-dependent DFT study on band gaps and effective conjugation lengths of polyacetylene, polyphenylene, polypentafulvene, polycyclopentadiene, polypyrrole, polyfuran, polysilole, polyphosphole and polythiophene*, Macromolecules 35 (2002), pp. 1109–1115.

[12] M.A. De Oliveira, H.A. Duarte, J.M. Pernaut, and W.B. De Almeida, *Energy gaps of α,α-substituted oligothiophenes from semiemperical, ab initio, and density functional methods*, J. Phys. Chem. A 104 (2000), pp. 8256–8262.

[13] N. S. Sariciftci (ed.), *Primary Photoexcitations in Conjugated Polymers: Molecular Exciton Versus Semiconductor Band Model*, World Scientific, Singapore, 1997, pp. 1–17 and 559–583.

[14] A. Donat-Bouillud, L. Lévesque, Y. Tao, M. D'Iorio, S. Beaupré, P. Blondin, M. Ranger, J. Bouchard, and M. Leclerc, *Light-emitting diodes from fluorene-based π-conjugated polymers*, Chem. Mater. 12 (2000), pp. 1931–1936.

[15] E. Lim, B.-J. Jung, and H.-K. Shim, *Synthesis and characterization of a new light-emitting fluorene-thieno[3,2-b]thiophene-based conjugated copolymer*, Macromolecules 36 (2003), pp. 4288–4293.

[16] E. Lim, B.-J. Jung, J. Lee, H.-K. Shim, J.-I. Lee, Y.S. Yang, and L.-M. Do, *Thin-film morphologies and solution-processable field-effect transistor behavior of a fluorene-thieno[3,2-b]thiophene-based conjugated copolymer*, Macromolecules 38 (2005), pp. 4531–4535.

[17] W. Tang, L. Ke, L. Tan, T. Lin, T. Kietzke, and Z.-K. Chen, *Conjugated copolymers based on fluorene-thieno[3,2-b]thiophene for light-emitting diodes and photovoltaic cells*, Macromolecules 40 (2007), pp. 6164–6171.

[18] E. Lim, Y.M. Kim, J.-I. Lee, B.-J. Jung, N.S. Cho, J. Lee, L.-M. Do, and H.-K.J. Shim, *Relationship between the liquid crystallinity and field-effect-transistor behavior of fluorene-thiophene-based conjugated copolymers*, Polym. Sci. Part A Polym. Chem. 44 (2006), pp. 4709–4721.

[19] G. Klaerner and R.D. Miller, *Polyfluorene derivatives: effective conjugation lengths from well-defined oligomers*, Macromolecules 31 (1998), pp. 2007–2009.

[20] J.L. Brédas, R. Silbey, D.S. Boudreaux, and R.R. Chance, *Chain-length dependence of electronic and electrochemical properties of conjugated systems: polyacetylene, polyphenylene, polythiophene, and polypyrrole*, J. Am. Chem. Soc. 105 (1983), pp. 6555–6559.

[21] M.J. Frisch, G.W. Trucks, H.B. Schlegel, G.E. Scuseria, M.A. Robb, J.R. Cheeseman, J.A. Montgomery, Jr, T. Vreven, K.N. Kudin, J.C. Burant et al. *Gaussian 03, Revision B.05*, 05, Gaussian, Inc., Pittsburgh, PA, 2003.

[22] D. Chakrabory and J.B. Lagowski, *Configuration interaction study of singlet excited state of thiophene and its cyano derivative oligomers*, J. Chem. Phys. 115 (2001), pp. 184–194.

[23] A. Curioni, W. Andreoni, R. Treusch, F.J. Himpsel, E. Haskal, P. Seidler, C. Heske, S. Kakar, T. van Buuren, and L.J. Terminello, *Atom-resolved electronic spectra for Alq^3 from theory and experiment*, Appl. Phys. Lett. 72 (1998), pp. 1575–1577.

[24] J.-F. Wang, J.-K. Feng, A.-M. Ren, X.-D. Liu, Y.-G. Ma, P. Lu, and H.-X. Zhang, *Theoretical studies of the absorption and emission properties of the fluorene-based conjugated polymers*, Macromolecules 37 (2004), pp. 3451–3458.

[25] M. Belletete, S. Beaupre, J. Bouchard, P. Blondin, M. Leclerc, and G. Durocher, *Theoretical and experimental investigation of spectroscopic and photophysical properties of fluorene-phenylene and fluorene-thiophene derivatives: precursors of light-emitting polymers*, J. Phys. Chem. B 104 (2000), pp. 9118–9125.

[26] J. Teetsov and M.A. Fox, *Photophysical characterization of dilute solutions and ordered thin films of alkyl-substituted polyfluorenes*, J. Mater. Chem. 9 (1999), p. 2117.

[27] G. Zeng, W.L. Yu, S.J. Chua, and W. Huang, *Spectral and thermal spectral stability study for fluorene-based conjugated polymers*, Macromolecules 35 (2002), pp. 6907–6914.

[28] J. Hwang, E.-G. Kim, J. Liu, J.-L. Bredas, A. Duggal, and A. Kahn, *Photoelectron spectroscopic study of the electronic band structure of polyfluorene and fluorene-arylamine copolymers at interfaces*, J. Phys. Chem. C 111 (2007), pp. 1378–1384.

[29] P. Chen, G. Yang, T. Liu, T. Li, M. Wang, and W. Huang, *Optimization of opto-electronic property and device efficiency of polyfluorenes by tuning structure and morphology*, Polym. Int. 55 (2006), pp. 473–490.

[30] S. Grimme and M. Parac, *Substantial errors from time-dependent density functional theory for the calculation of excited states of large systems*, ChemPhysChem 4 (2003), pp. 292–294.